INTERNATIONAL JOURNAL OF CLIMATOLOGY
Int. J. Climatol. (2017)
Published online in Wiley Online Library
(wileyonlinelibrary.com) DOI: 10.1002/joc.5265

Royal Meteorological Society

Dimming in Iran since the 2000s and the potential underlying causes

Babak Jahani,[a*] Yagob Dinpashoh[a] and Martin Wild[b]
[a] *Department of Water Resources, University of Tabriz, Iran*
[b] *Institute for Atmospheric and Climate Science, ETH Zurich, Switzerland*

ABSTRACT: This study investigates the spatio-temporal variations of global solar radiation and its relationships with cloud cover (CC) during 1998–2015 in Iran, where no previous information about the variations of solar radiation based on direct measurements exists. The variations in the mentioned variables were detected using a modified Mann–Kendall trend test and the magnitudes of trends were estimated by using the Theil–Sen's slope estimator method. A widespread dimming with a magnitude of about −4.3 and −1.7% per decade is found under all- and clear-sky conditions in Iran since the 2000s (median over nine observation sites). A significant increase in CC was observed at most of the stations studied, at 20.0% per decade (median over nine sites). The decrease in the amount of all-sky global solar radiation seems to have occurred as a combined effect of aerosol and CC increase over Iran. However, in the south of Iran and at the station Tehran dimming appears to be mostly due to an increase in the amount of aerosol loadings.

KEY WORDS cloud cover; global solar radiation; Iran; Mann–Kendall; Sen's slope estimator; trend analysis

Received 13 April 2017; Revised 11 July 2017; Accepted 4 August 2017

1. Introduction

Solar radiation that reaches the Earth surface (R_s) (also known as global solar radiation) plays a key role in various natural processes such as the hydrological cycle (Wild *et al.,* 2005; Xia *et al.,* 2006; Wild, 2009; Dagon and Schrag, 2016; Manara *et al.,* 2016; Jahani *et al.,* 2017). For example, R_s provides the energy for photosynthesis, evaporation, evapotranspiration, cloud formation, snow melt, etc. (Kun *et al.,* 2006; Wild *et al.,* 2015a; Dagon and Schrag, 2016; Huber *et al.,* 2016). Therefore, it is considered as one of the most important inputs of hydrological, irrigation scheduling and crop growth models (Aladenola and Madramootoo, 2014; Jahani *et al.,* 2016; Jahani *et al.,* 2017; Quej *et al.,* 2017; Wang *et al.,* 2017). Furthermore, R_s is also a renewable clean source of energy, which has received increasing attention recently, because it can be exploited without bearing any harm to nature and is also an alternative for fossil fuels (Viorel, 2008; Zekai, 2008; Demirhan and Atilgan, 2015; Wild *et al.,* 2015a; Wild *et al.,* 2015b; El Mghouchi *et al.,* 2016). Consequently, any changes in R_s affect different aspects of wild life, human life and natural processes on Earth.

The amount of R_s received at a certain location on the Earth is affected by various factors, but in general, R_s variations can either be caused by variations in the amount of solar radiation reaching the top of the atmosphere (R_a) or by changes in the transparency of the atmosphere (Wild, 2009). Studies show that variations in the quantity of R_a are negligible compared to the variations observed at the Earth's surface (Wild, 2009). Therefore, variations in the amount of R_S are mainly caused by changes in the transparency of the atmosphere. The transparency of the atmosphere may change as a result of increasing/decreasing amounts of man-made or natural aerosols, volcanic eruptions, changes in the cloud cover (CC) and its type, etc. (Power, 2003; Pinker *et al.,* 2005; Qian *et al.,* 2006; Ramanathan *et al.,* 2007; Dong *et al.,* 2012; Soni *et al.,* 2012; Lindfors *et al.,* 2013; Chin *et al.,* 2014; Mateos *et al.,* 2014; Calbo *et al.,* 2016; Manara *et al.,* 2016; Qian, 2016; Wang *et al.,* 2016; Yang *et al.,* 2016; Tang *et al.,* 2017). The relevant reports with respect to R_S variations suggest that the amount of R_S has changed in the recent decades at many observation sites all around the world (Pinker *et al.,* 2005; Wild *et al.,* 2005; Wild, 2009; Müller *et al.,* 2014; Sanchez-Lorenzo *et al.,* 2015; Wild *et al.,* 2015b; Von Schuckmann *et al.,* 2016). In Europe, for instance, R_S has decreased by more than 10% at some measurement sites from 1960 to 1990 (Ohmura and Lang, 1989). R_S has decreased in China from 1954 to 2001 (Qian *et al.,* 2006). Xia *et al.* (2006) also detected significant downward and upward trends in the quantity of R_S in China, in the periods of 1961–1980 and 1984–2000, respectively. However, it is worth mentioning that inhomogeneities in the Chinese records due to instrument replacements at many of the sites in the early 1990s may have introduced spurious trends (Tang *et al.,* 2010; Wang *et al.,* 2012; Wang and Wild, 2016). The results of a study carried out by Soni *et al.* (2012) also showed a

* Correspondence to: B. Jahani, Department of Water Resources, University of Tabriz, 29 Bahman Ave., Daneshgah Square, Tabriz, Iran. E-mail: bob.jahan@gmail.com

decline in the annual amount of R_S between 1971 and 2005, in India. Kumari *et al.* (2007) also reported an averaged decline of about 0.86 W m^{-2} per year for the period of 1981–2004 in India. Moreover, findings of Wild *et al.* (2005) showed that despite that global dimming (decrease in the quantity of R_S) had taken place in the Northern Hemisphere between the 1950s and 1980s, a widespread brightening (increase in the quantity of R_S) was observed since the 1980s. This fact has also been highlighted by other researchers focusing on both worldwide and regional trends of R_S (Alpert *et al.,* 2005; Sanchez-Lorenzo and Wild, 2012; Sanchez-Lorenzo *et al.,* 2013, 2015; Chiacchio *et al.,* 2015; Wild *et al.,* 2015b; Manara *et al.,* 2016; Wang *et al.,* 2016; Sanchez-Lorenzo *et al.,* 2017). A positive significant ($p < 0.05$) trend of about 9–18 W m^{-2} per decade was also observed in Hawaii during the dry season (May–October) since the 1980s (Longman *et al.,* 2014). Similarly, an average upward trend of about 3.9 W m^{-2} per decade was reported for the period of 1985–2010 in Spain (Sanchez-Lorenzo *et al.,* 2013, 2014). Calbo *et al.* (2016) also observed a significant upward trend in the mean annual R_S records of 1987–2014 in Girona (Spain). Rahimzadeh *et al.* (2015) analysed the duration of sunshine hours in Iran for the period of 1961–2009 and reported that despite an increase in the rate of sunshine hours from the early 1980s to the end of 20th century, a renewed dimming is observed during the 2000s in Iran, with a sharp drop in 2009.

However, the exact reasons for these decadal changes in R_S in different parts of the world are not completely clear yet. According to our best knowledge, variations in the quantity of directly measured R_S (rather than sunshine hours) have not been studied in Iran previously. The main objective of this study is therefor to analyse the spatial and temporal variations of directly measured R_S in Iran and to investigate how these variations in R_S would be related to changes in CC variability in Iran in the 2000s.

2. Materials and methods

2.1. Data

Despite that there are more than 330 synoptic stations all over Iran, recording a range of meteorological parameters (Rahimzadeh *et al.,* 2015), R_S is not widely recorded at most of the synoptic stations of the network of Islamic Republic of Iran Meteorological Organization (IRIMO). The radiation network of Iran consists of 23 synoptic stations by now and was first established in 1992 (merely 13 of the stations have been operational since 1992). Besides, data gaps and instrumental errors (outliers) between 1992 and 1997 make the 1992–1997 R_S measurements of these stations unreliable. In this study, in order to investigate the relationships between the changes in CC and R_S in Iran, the hourly records of R_S (W m^{-2}) and CC (octa) for the 23 radiation network stations of Iran were obtained from IRIMO (Jahani *et al.,* 2017). Despite the fact that CC has been recorded at all of these stations since 1961, these hourly records were uniformly available only after around 1980. The hourly R_S and CC data were initially transformed to the daily means by averaging the recorded values of them at 0900, 1200, 1500 and 1800 h (GMT +03:30). The daily values of CC were then utilized to determine the occurrence of the clear-sky conditions (CSCs) to generate the time series of number of days with CSCs, and CSC is defined as a day with a daily amount of CC less than 1 octa. Furthermore, the daily values of R_S were checked for potential outliers by estimating the clearness index (K_r) as the ratio of R_S to extraterrestrial solar radiation. Then the data with respect to the days with an amount of K_r less than 0.03 or more than 1 were removed (Allen *et al.,* 1998; Tang *et al.,* 2011; Jahani *et al.,* 2017). In addition, the metadata of the stations was checked, in order to analyse whether coordinates and elevation of the stations have changed over the study period or not. After that, based on the availability of uniform R_S and CC for 1998–2015 an overall number of nine stations were selected across Iran (Table 1 and Figure 1). These stations are mainly located at the metropolitan cities of Iran. Furthermore, in order to determine to what extent the R_S variability in Iran in the 2000s may depend on changes in CC, the variations in the time series of R_S under all-sky (ASR_S) and clear-sky (CSR_S) conditions were investigated. The daily ASR_S, CSR_S and CC data with respect to each station were averaged over every month, and the annual averages were similarly obtained by averaging the monthly values. Specifically, the monthly means of CSR_s were calculated when at least two clear-sky daily values were available in a month (Manara *et al.,* 2016), and in some a few particular cases where not a sufficient number of days with CSC in a given month were available to establish a mean monthly value of CSR_s, in order to avoid unreal/artificial trends, the climatological mean of the corresponding month was considered as the mean monthly value of that month. By doing so, the annual time series of CSR_s were always generated by averaging over the entire 12 months of the year, and thereby the introduction of spurious trends due to unevenly distributed clear-sky days was prevented. The annual and monthly values were then utilized for further analysis.

The latitudes of the stations selected varied between 27.21 and 38.12°N, the longitudes of them were between 45.06 and 60.90°E and the altitudes of the stations varied between 9.8 and 1549.1 masl. According to Figure 1, elevation varies considerably in Iran, mostly due to the existence of the Alborz and Zagros Mountains. Four of the stations selected were located along the Zagros Mountains (Figure 1, stations Tabriz, Urmia, Sanandaj and Kermanshah) and one was located along the Alborz Mountains (station Tehran). It is also worth to mention that the station Urmia is located around the shorelines of Urmia Lake, which is known as the second greatest hypersaline lake of the world (Stone, 2015).

2.2. Trend analysis

In this study, in order to analyse the temporal variations of R_S in Iran, the non-parametric Mann–Kendall (MK) (Mann, 1945; Kendall, 1975) method was utilized. This

Table 1. Details of the nine stations selected in this study.

Station name	Latitude (°N)	Longitude (°E)	Altitude (masl)	Time period	
				R_s	CC
Ahvaz	31.34	48.74	22.50	1993–2015	1961–2015
Bandarabbas	27.21	56.37	9.80	1993–2015	1956–2015
Kermanshah	34.35	47.15	1318.50	1993–2015	1961–2015
Mashhad	36.24	59.63	999.20	1993–2015	1951–2015
Sanandaj	35.25	47.01	1373.40	1993–2015	1961–2015
Tehran	35.80	51.49	1549.10	1993–2015	1951–2015
Tabriz	38.12	46.24	1361.00	1993–2015	1956–2015
Urmia	37.66	45.06	1328.00	1993–2015	1951–2015
Zahedan	29.47	60.90	1370.00	1993–2015	1951–2015

Note that masl stands for 'meters above average sea level' (R_s is global solar radiation and CC is cloud cover).

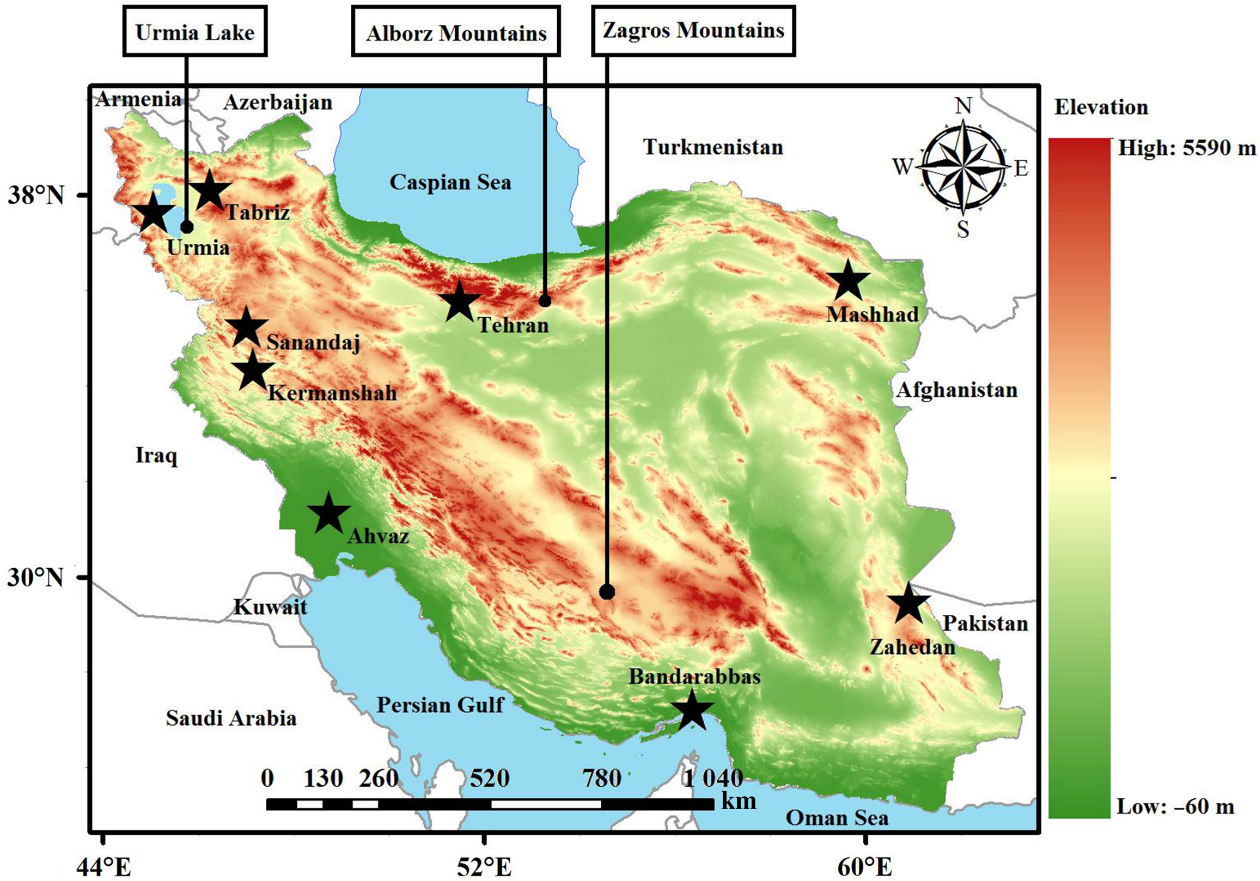

Figure 1. Geographical features of Iran and locations of selected stations. [Colour figure can be viewed at wileyonlinelibrary.com].

approach has some advantages. First, it does not require the data to be normally distributed (Tabari and Hosseinizadeh, 2011). Second, this procedure has a low sensitivity to abrupt breaks due to data gaps in the time series (Jaagus, 2006). Moreover, this method is not sensitive to outliers. According to this test, the null hypothesis H_0 states that there is no trend in the data $(x_1, \ldots, x_n)$. The alternative hypothesis H_1 in a two-sided test is that there is a significant trend in the observations (Tabari and Hosseinizadeh, 2011). The MK-trend test is initially carried out by computing the S statistics using Equation (1) (Dinpashoh *et al.*, 2011).

$$S = \sum_{i=1}^{n-1} \sum_{j=i+1}^{n} \operatorname{sgn}\left(x_j - x_i\right) \quad (1)$$

where, n is the number of observations, x_j and x_i are the jth and ith observations, respectively, and sgn(.) refers to the sign function, which is defined as

$$\operatorname{sgn}\left(x_i - x_j\right) = \begin{cases} 1 & \text{if } \left(x_j - x_i\right) > 0 \\ 0 & \text{if } \left(x_j - x_i\right) = 0 \\ -1 & \text{if } \left(x_j - x_i\right) < 0 \end{cases} \quad (2)$$

Under the assumption that the data is independent and identically distributed and $E(S) = 0$, the variance of S is

Table 2. Long-term means, SD and trend line slopes (β_s) of annual ASR_S, CC and CSR_S in Iran for 1998–2015.

Station name	Long-term means (SD)			Trend line slope (% per decade)		
	ASR_S ($W\,m^{-2}$)	CSR_S ($W\,m^{-2}$)	CC (octa)	ASR_S	CSR_S	CC
Ahvaz	202.1 (7.6)	215.6 (7.4)	2.2 (0.4)	−0.8	**−3.5***	**34.2****
Bandarabbas	203.8 (5.2)	220.0 (4.9)	1.9 (0.3)	**−2.5***	−1.3	**20.0**
Kermanshah	203.9 (15.1)	229.6 (14.5)	2.8 (0.4)	**−4.8**	**−6.1****	**28.6****
Mashhad	208.6 (15.9)	232.6 (10.5)	3.0 (0.4)	**−5.7****	−0.9	**21.2****
Sanandaj	208.9 (9.0)	239.2 (8.7)	2.8 (0.2)	**−3.9**	−2.1	**7.7****
Tehran	198.8 (9.7)	229.0 (8.9)	3.6 (0.3)	**−4.3**	**−4.9****	**−6.1***
Tabriz	164.1 (10.9)	209.3 (6.0)	3.5 (0.3)	**−4.2****	−1.2	**9.4****
Urmia	181.9 (22.2)	206.5 (20.5)	3.1 (0.3)	−8.2	−0.5	**19.2****
Zahedan	179.9 (28.5)	208.7 (15.2)	2.0 (0.4)	−6.5	−1.7	**53.3****
Median of slopes				−4.3	−1.7	20.0

Note that the values of β indicate trend line slopes. Also, significance of the trend at 0.1 level is shown by bold values. *Significance of trend at 0.05 level. **Significance of trend at 0.01 level.

calculated as follows:

$$V(S) = \frac{n(n-1)(2n+5) - \sum_{i=1}^{m} t_i\left(t_i - 1\right)\left(2t_i + 5\right)}{18} \tag{3}$$

where, m is the number of groups of tied ranks and t_i is the number of data points in the ith tied group. And finally, the MK statistics, denoted by Z, is calculated as

$$Z = \begin{cases} \frac{(S-1)}{\sqrt{V(S)}} & \text{if } S > 0 \\ 0 & \text{if } S = 0 \\ \frac{(S+1)}{\sqrt{V(S)}} & \text{if } S < 0 \end{cases} \tag{4}$$

If $|Z| \leq Z_{1-\alpha/2}$ then the null hypothesis of no trend at the significance level of α is accepted. Otherwise, the H_0 is rejected and the H_1 at the significance level of α is accepted. In this study, the MK test was conducted at 10% ($\alpha = 0.1$), 5% ($\alpha = 0.05$) and 1% ($\alpha = 0.01$) level of significance.

Furthermore, in order to analyse the magnitude of the trends, the Theil–Sen's slope estimator was calculated (Theil, 1950; Sen, 1968; Dinpashoh *et al.,* 2011). The Theil–Sen's slope (β) is calculated as follows:

$$\beta = \text{Median}\left(\frac{x_j - x_l}{j - l}\right) \quad \forall 1 < l < j \tag{5}$$

However, there is an important limitation in using the MK method: In the case of presence of significant lag-1 auto-correlation coefficients (r_1) in the examined time series, this method leads to misleading results. This is due to the fact that the effect of significant r_1 on trend statistic is a major source of uncertainty. Thus, in order to eliminate the influence of significant r_1 in the series of data in the 90% confidence interval, the series were pre-whitened (Dinpashoh *et al.,* 2011) and then the series treated this way were subjected to trend analysis. According to Kumar *et al.* (2009) the newly adjusted time series can be obtained using the Equations (6)–(8).

$$x'_i = x_i - (\beta \times i) \tag{6}$$

$$y'_i = x'_i - \left(r_1 \times x'_{i-1}\right) \tag{7}$$

$$y_i = y'_i + (\beta \times i) \tag{8}$$

where, r_1 is the lag-1 autocorrelation coefficient of the time series. Finally, y_i ($i = 1, 2, \ldots, n$) is then subjected to the conventional MK test.

3. Results

3.1. All-sky solar radiation

The values of β as well as the long-term mean and standard deviation (SD) for the variables ASR_S, CSR_S and CC at each of the stations selected are provided in Table 2. The observed long-term mean annual values of ASR_S ranged between 164.1 $W\,m^{-2}$ at Tabriz and 208.9 $W\,m^{-2}$ at Sanandaj. The station Bandarabbas also had the smallest inter-annual variability, with a SD equal to 5.2 $W\,m^{-2}$. The station Zahedan (SD: 28.5 $W\,m^{-2}$) in contrast had the greatest inter-annual variability.

The seasonal variations of ASR_S in terms of long-term monthly averages at each of the stations studied for 1998–2015 are elaborated in Figure 2. From this figure, it can be seen that the maximum and minimum amounts of ASR_S are received in June and December, respectively. Furthermore, this figure also shows that the amount of ASR_S received between June and September (during spring and summer) encompass a great proportion of the total annual ASR_S received in Iran. This implies that any changes in the factors affecting transparency of the atmosphere during spring and summer would have stronger influences on the amount of total annual ASR_S received in Iran.

The results of the trend analysis for ASR_S, summarized in Table 2, show an evident and wide-spread decrease (either significant or non-significant) in the amount of ASR_S in Iran between 1998 and 2015. The magnitude of this decline in the amount of ASR_S varied between −8.2% per decade at the station Urmia and −0.8% per decade at the station Ahvaz for 1998–2015. The long-term

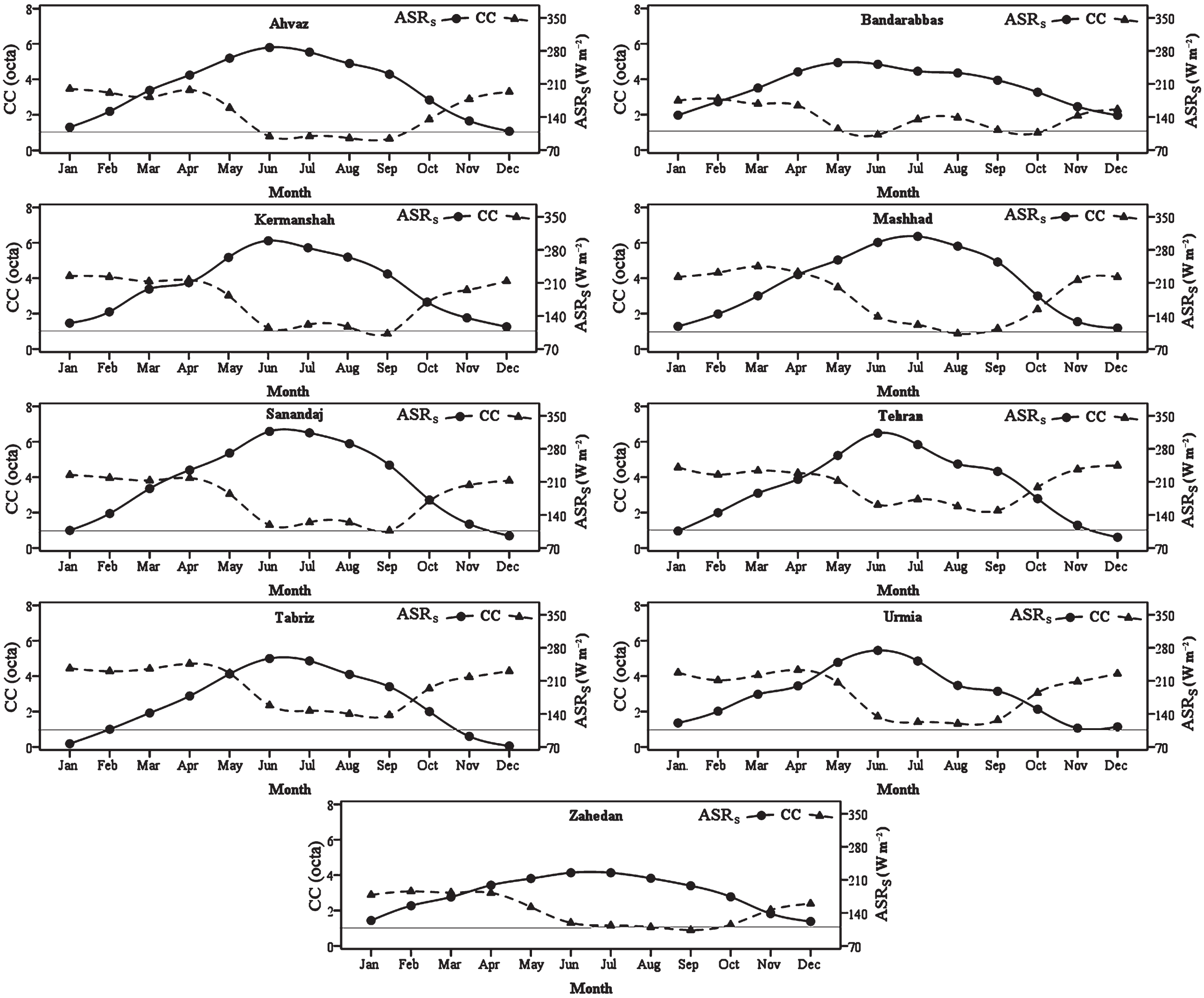

Figure 2. Long-term monthly averages of ASR$_S$ (right vertical axis) and CC (left vertical axis) for 1998–2015 at nine sites in Iran.

annual means of the stations Urmia and Ahvaz were equal to 181.9 W m^{-2} (SD: 20.5 W m^{-2}) and 202.1 W m^{-2} (SD: 7.6 W m^{-2}), respectively. The median of the decline in the trend slopes was equal to −4.3% per decade for the period of 1998–2015. A statistically significant decline in the amount of ASR$_S$ was observed at six of the nine stations studied. These significant decreases were observed at the stations Bandarabbas (at the 5% level), Kermanshah (10%), Mashhad (1%), Sanandaj (10%), Tehran (10%) and Tabriz (1%). Among those, the stations Mashhad and Bandarabbas had the most and least steep significant trends at −5.7 and −2.5% per decade during the 2000s, respectively. The location of these stations is illustrated in Figure 3. As can be seen from Figure 3, among the stations located in the north of Iran, merely one station (Urmia) does not show a significant downward trend at the 10% significance level. In contrast, among the stations located in the south of Iran, a significant decreasing trend (at the 10% level) was only observed at the station Bandarabbas, which is a coastal station. The time series of observed ASR$_S$ for the period of 1998–2015 at each of the nine stations considered in this study, together with fitted-trend lines, are illustrated in Figure 4. According to this figure, despite the fact that the fitted-trend line shows an overall significant decline since the 2000s, ASR$_S$ at the station Mashhad does not seem to undergo monotonic variations during 1998–2015. As these time-series show (Figure 4), ASR$_S$ has increased between 1998 and 2007 and decreased during 2007–2015. Figure 4 also shows a transition from dimming to brightening at the station Zahedan (located in the southeast of Iran) in the year 2006. However, the overall trend of ASR$_S$ during 1998–2015 seems to be downward.

The box plots illustrated in Figure 5 provide information about the monthly trend slopes detected in the ASR$_S$ time series at the nine stations studied during the 2000s. According to this figure, a mostly homogeneous decrease in the amount of ASR$_S$ has been observed in almost all months of year. This implies that the observed downward trends in the mean annual values of ASR$_S$ do not originate from a decline in ASR$_S$ in a certain month of the year, but come from widespread decreases in almost all months of the year. The sharpest and weakest relative declines, in terms of median of β_s, were observed in November and August, respectively.

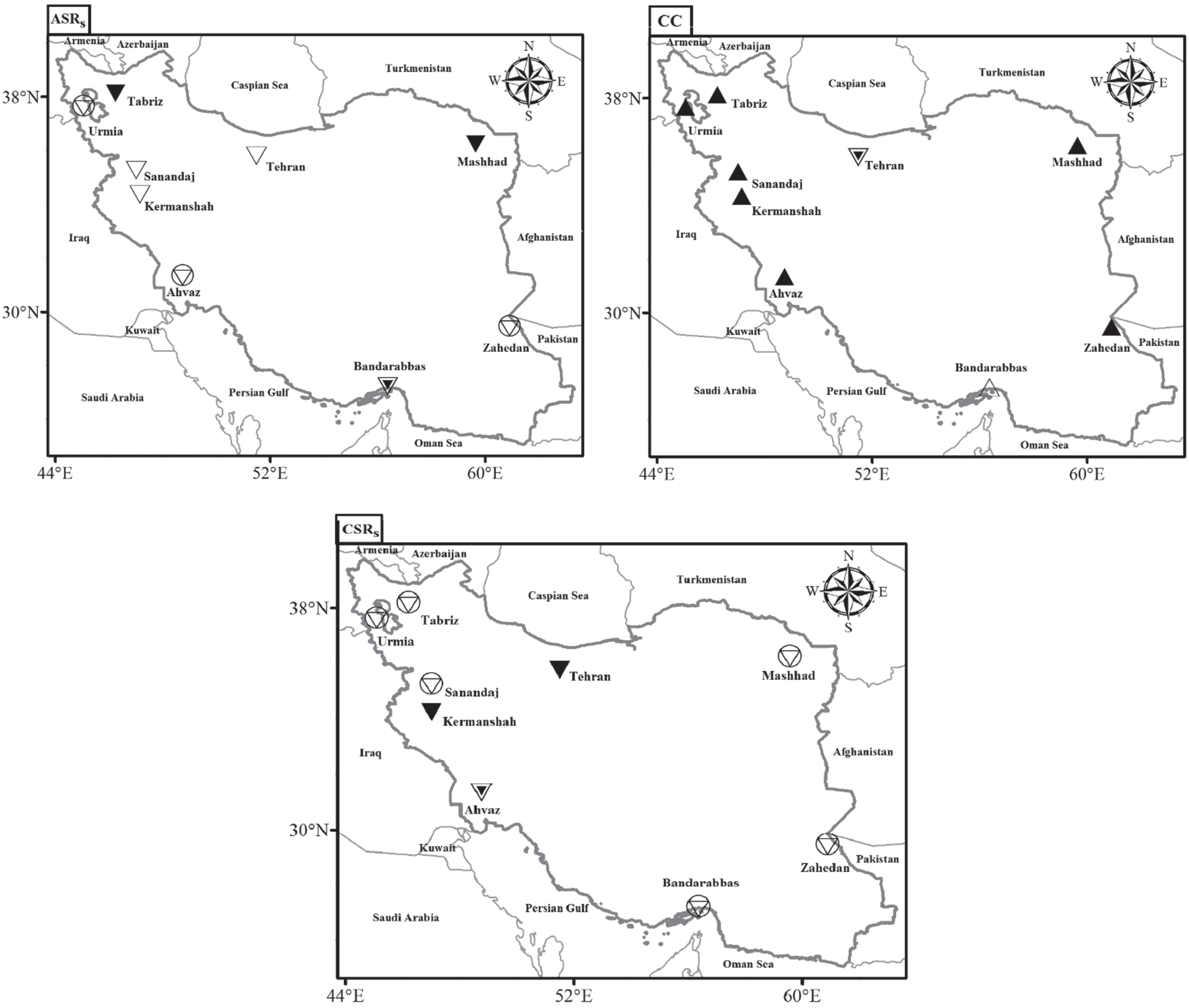

Figure 3. Location of the sites in Iran with decreasing (down-pointing triangles) and increasing (up-pointing triangles) non-significant (⊽⊼) as well as significant trends at 10 (▽△), 5 (⧨⧩) and 1% (▼▲) levels for annual ASR$_S$, CSR$_S$ and CC time series (1998–2015).

3.2. Cloud cover

The long-term mean annual values of CC provided in Table 2 show that CC varies notably in terms of magnitude in Iran. The stations Tehran with a long-term mean annual value of CC = 3.6 octa (SD: 0.3 octa) and Bandarabbas with CC = 1.9 octa (SD: 0.3 octa) had the greatest and smallest long-term averaged values of CC among the stations studied, respectively. In terms of geographical location, these two stations differ a lot (Figure 1). Moreover, the smallest inter-annual variability in CC, in terms of SD, belonged to the station Sanandaj (SD: 0.2 octa). The stations Ahvaz, Kermanshah, Mashhad and Zahedan with a SD equal to 0.4 octa, almost equally had the largest inter-annual variability among the nine stations studied. In addition, a comparison between the long-term averaged values of CC observed at the stations studied shows that clouds are less frequent in the south of Iran. The seasonal distribution of CC provided in Figure 2 indicates a fairly similar seasonal pattern of CC at all of the stations studied. According to Figure 2, CC is minimal during summer and maximal during winter in most of the stations. This reflects the fact that CC may have less effect on the transparency of the atmosphere during summer (when the greatest proportion of ASR$_S$ is received) in Iran.

According to Table 2, statistically significant trends were observed at all of the stations studied. Among them, eight were upward and one (station Tehran $\beta = -6.1\%$ per decade) was downward. The magnitude of these trends was between −6.1 and 53.3% per decade and also had a median value of about 20.0% per decade. Among the stations showing upward trends, the stations Zahedan with 53.3% per decade and Sanandaj with 7.7% per decade exhibited the steepest and weakest relative upward trends in CC. Among the stations located in the west of Iran, the stations Ahvaz with a β of 34.2% per decade and Sanandaj with a β of 7.7% per decade showed the steepest and weakest relative increases in CC during 1998–2015, respectively. Moreover, according to the time series of CC provided in Figure 6, a mostly monotonic increase in the amount of CC was observed at all of the stations studied

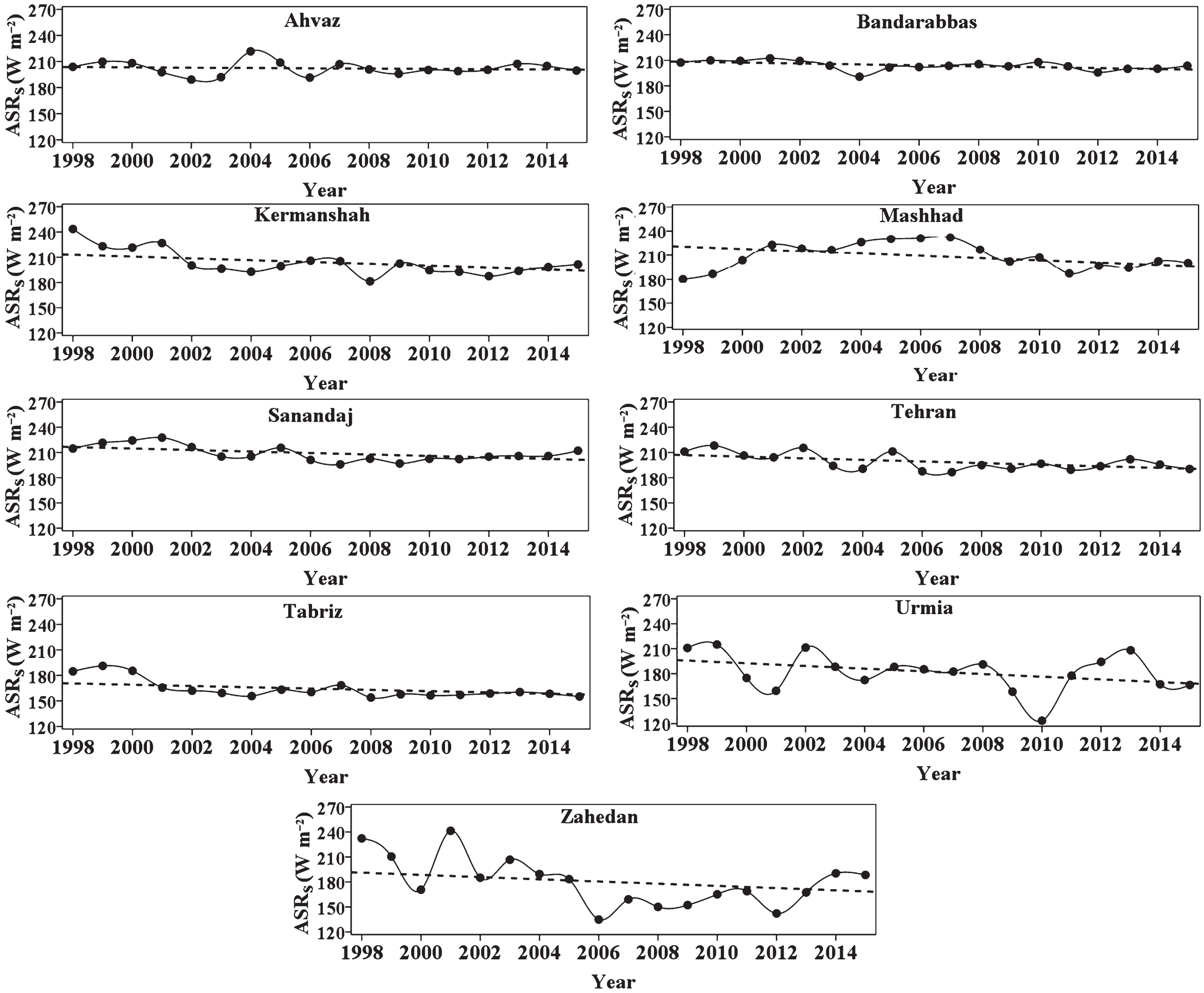

Figure 4. Mean annual ASR_S time series for 1998–2015 at each of the nine stations selected (note: the dashed line represents the trend line fitted through Sen's slope estimator approach).

except the station Mashhad. At this station, CC seems to have decreased during 1998–2008, but then increased during 2008–2015. Nevertheless, based on the trend statistics given in Table 2 and also the fitted-trend line shown in Figure 6, overall the amount of CC at the station Mashhad seems to have increased by 21.2% per decade between 1998 and 2015.

From the box plots of the trend slopes observed in the mean monthly time series of CC provided in Figure 5, it can be inferred that overall CC has increased in 10 months of the year in Iran. The median of the β_s also show a very weak relative decline in the amount of CC in December and January.

3.3. Relationships between ASR_S and CC

This section is dedicated to the comparison between the variations of mean annual ASR_S (dependent variable; the variable whose variation is being studied) and CC (independent variable; the variable which is used to explain how the magnitude of the dependent variable changes) in Iran. These relationships have been evaluated by using scatterplots, trend slopes (β_s) and correlation coefficients between ASR_S and CC.

A comparison between the trends observed in the annual averages of CC and ASR_S shows that these two variables have mostly varied in line with each other at almost all of the sites (except at the station Tehran) in 1998–2015. The correlations between annual mean CC and ASR_S (at all sites studied) shown in Figure 7 also show inverse relationships between these two variables (either significant or non-significant) at all of the stations studied between 1998 and 2015. However, significant correlations ($\alpha = 0.01$) were observed at merely three of the nine stations studied, namely Mashhad, Tabriz and Zahedan. These strong negative correlations between CC and ASR_S reveal the fact that the CC variations may substantially influence the inter-annual variability of ASR_s and that increases in the amount of CC may to some extent be considered as one of the potential drivers of the decrease in the amount of ASR_S received in some parts of Iran during 1998–2015. In addition, it is worth to mention that the lack of correlation detected between CC and ASR_S at some of the stations

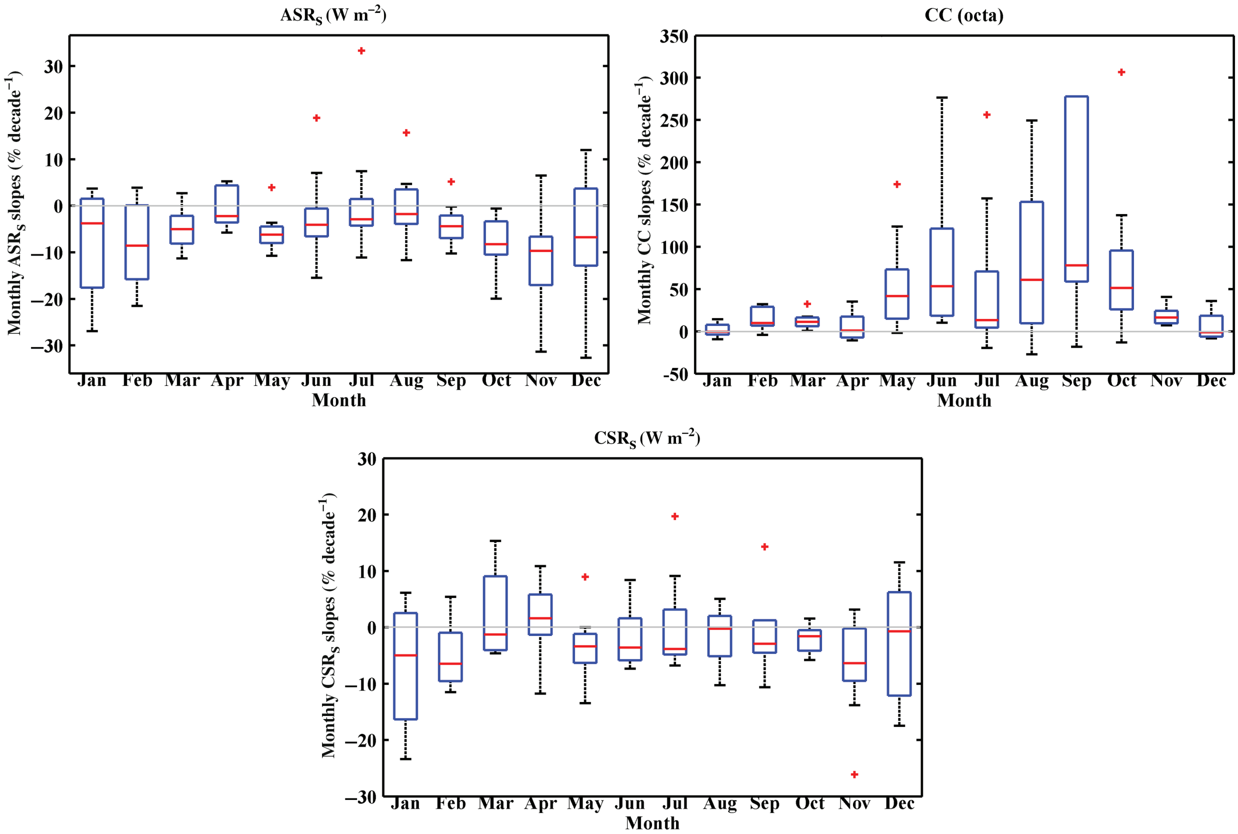

Figure 5. Box plots with respect to the magnitude of trends (β_s) observed in the monthly time series of ASR$_S$, CSR$_S$ and CC in Iran, during 1998–2015. The lines in the boxes represent the median of the β_s, the upper and lower edges of the boxes, respectively, show the range of β_s in the second and third quartiles, the dashed vertical lines above and below the boxes show the range of β_s at the first and fourth quartiles, respectively. [Colour figure can be viewed at wileyonlinelibrary.com].

may be due to the errors in CC observations, because the quantification of CC changes depends on human judgments. The scatterplots with respect to the mean annual time series of CC and ASR$_S$ at each of the stations studied are provided in Figure 8.

3.4. CSR$_S$ and its relationship with ASR$_S$

A comparison between the seasonal variation patterns of CSR$_S$ and ASR$_S$ is provided in Figure 9. According to this figure, apart from slight differences, CSR$_S$ seems to have a seasonal variability similar to ASR$_S$ in most of the stations studied, which is to be expected due to the seasonal variation of R_a. However, it is worth noticing that despite the fact that the amount of R_a is maximum during summer, the maximum amount of CSR$_S$ is received in May at the stations Urmia and Bandarabbas. This fact may be due to higher amount of aerosol and/or humidity stemming from evaporation from the Lake of Urmia (Stone, 2015; Shadkam *et al.,* 2016a; Shadkam *et al.,* 2016b; Moghaddasi *et al.,* 2017) and Persian Gulf during summer, which may lead to more scattering effects at the stations Urmia and Bandarabbas, respectively.

The results of the trend analysis of annual mean CSR$_S$ during 1998–2015 are represented in Table 2. This data show a widespread decrease in CSR$_S$ with a magnitude of about −1.7% per decade (median of the slopes observed at the sites) in Iran during the study period, which is in line with the variations of ASR$_S$ in Iran during the mentioned period. According to Table 2, the magnitude of the trends observed in CSR$_S$ (either significant or non-significant) ranged between −0.5 (Urmia) and −6.1% per decade (Kermanshah). Statistically significant declines in the amount of CSR$_S$ were observed at the three of the nine stations studied. These stations were Ahvaz ($\beta = -3.5\%$ per decade), Kermanshah ($\beta = -6.1\%$ per decade) and Tehran ($\beta = -4.9\%$ per decade). Among them, two were significant at the 1% level (Tehran and Kermanshah) and one (Ahvaz) was significant at the 5% level. According to the data provided in Figure 3, the stations Ahvaz and Kermanshah are located in the west and the station Tehran is in the north of Iran. A comparison between the anomalies of CSR$_S$ and ASR$_S$ at each of the stations studied during 1998–2015 has been provided in Figure 10. According to this figure, the transition from brightening to dimming, which was observed in ASR$_S$ anomalies at the station Mashhad seems not evident in those of CSR$_S$. In contrast, at the station Zahedan, Figure 10 shows a transition from dimming to brightening in CSR$_S$ in the year 2006, which is in line with what was observed in ASR$_S$. However, it is worth to mention that ASR$_S$ seems to have varied more considerably during the dimming and brightening periods, in comparison with CSR$_S$ at this station.

From the information provided in Figure 7 it can also be seen that strong positive correlations (either significant

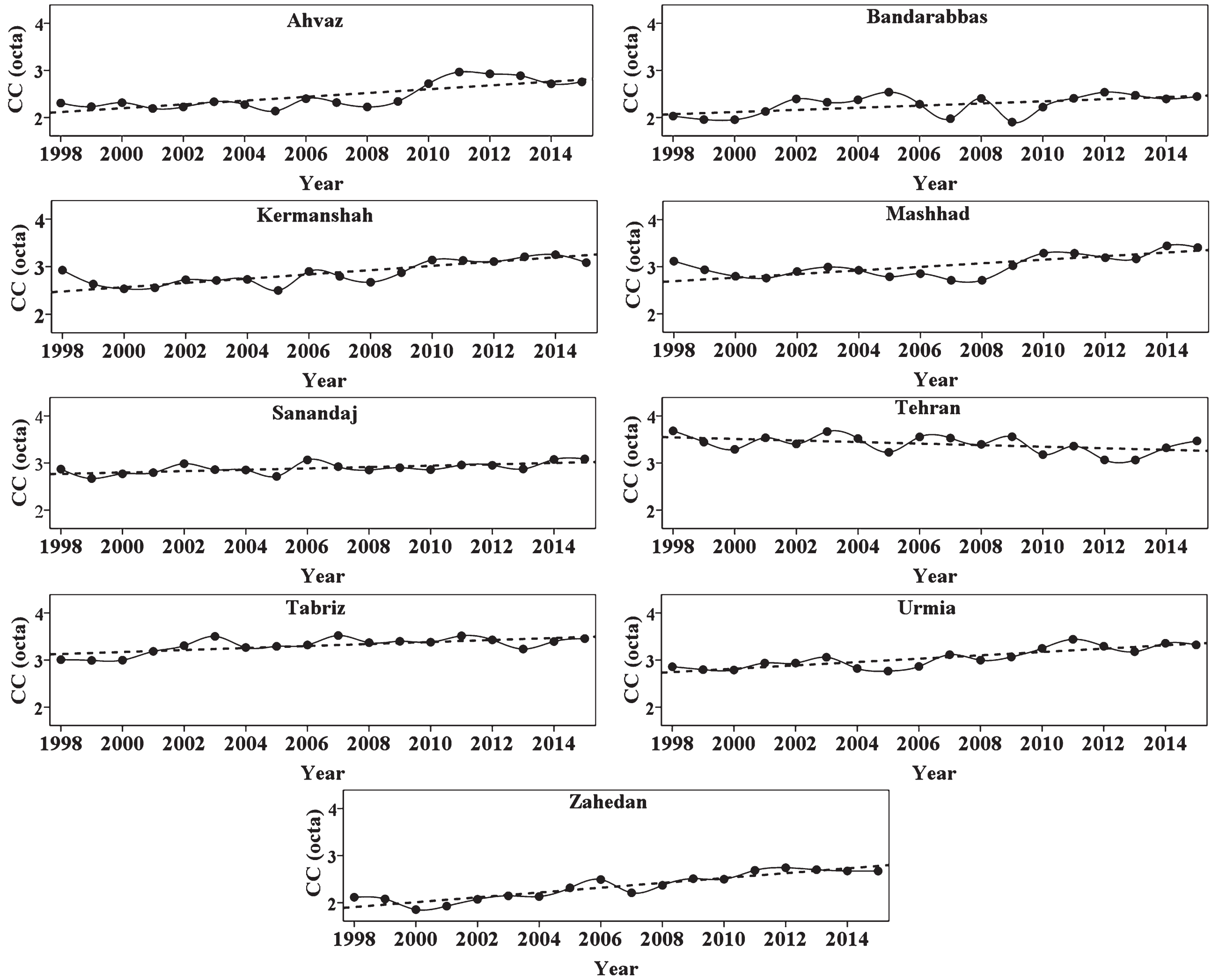

Figure 6. Mean annual CC time series for 1998–2015 at each of the nine stations selected (note: the dashed line represents the trend line fitted through Sen's slope estimator approach).

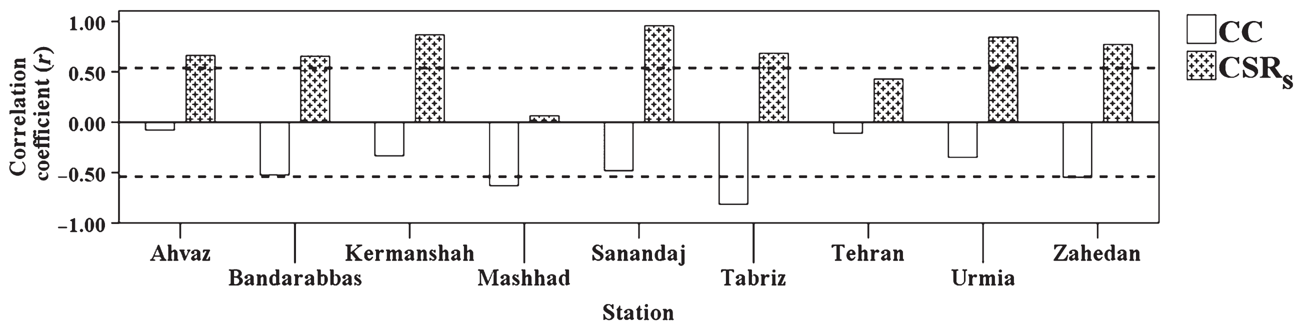

Figure 7. Correlation coefficients (r) between annual means of ASR_S and the corresponding variables CC and CSR_S at each of the nine stations studied (note: the dashed lines indicate the critical values of r at 1% ($\alpha = 0.01$) level of significance).

or non-significant) were observed between the annual values of ASR_S and CSR_S at almost all of the sites studied, except the station Mashhad. Among those, seven were significant at the 1% level. The lack of strong correlation detected between ASR_S and CSR_S at the station Mashhad supports the fact that variations of ASR_S observed at this station during the 2000s may not mainly originate from the variations detected in CSR_S. In contrast, the strong correlations (either significant or non-significant) observed at the other stations highlight the fact that the variations in aerosols loading and/or other natural factors affecting CSR_S may play an important role in the variations of ASR_S at eight of the stations studied. The scatterplots with respect to the mean annual time series of CSR_S and ASR_S during 1998–2015 are shown in Figure 11.

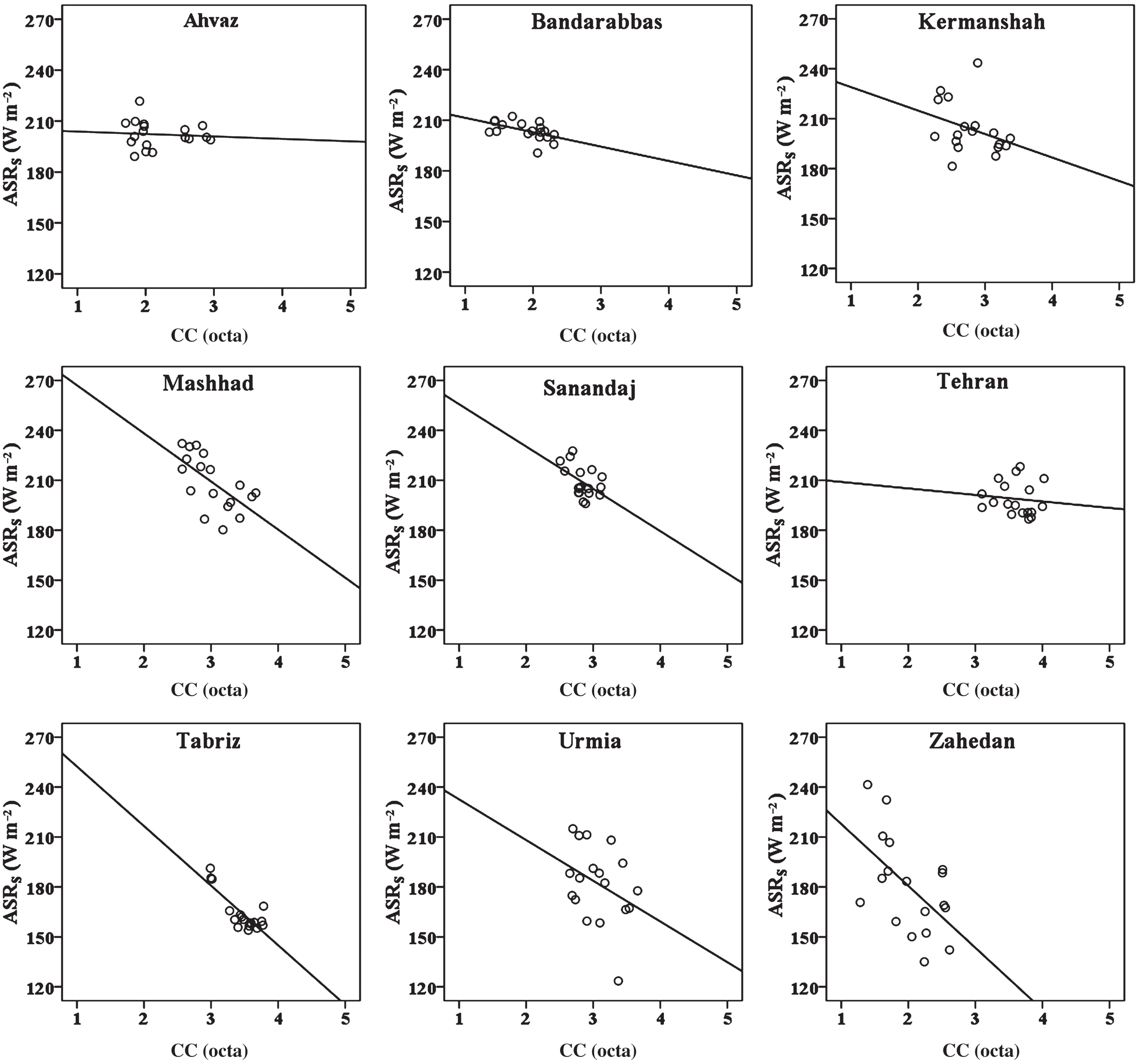

Figure 8. Scatterplots of the mean annual values of ASR_S *versus* CC observed at each of the stations studied (note: the solid line represents the least square line fitted between the ASR_S and CC observations).

The box plots shown in Figure 5 provide information about the trend slopes observed in the monthly time series of CSR_S at the nine stations studied between 1998 and 2015. This figure shows that CSR_S has decreased in more than half of the stations studied in almost all months of the year except in April.

4. Discussion

The main objective of this study was to analyse spatio-temporal variations of R_s based on direct measurements of incoming R_s fluxes in Iran since the 2000s, and also to investigate how these variations in R_s may be related to changes in CC. Overall, the mean annual time series of ASR_S and CSR_S measurements at the nine stations studied reveal a widespread and evident dimming phenomenon in Iran since the 2000s, where no previous information about the variations of R_s based on direct measurements exists. The magnitudes of these declines in the amount of ASR_S and CSR_S were −4.3 and −1.7% per decade (in terms of median), respectively. The decrease in the amount of ASR_S received in Iran since the 2000s also supports the results obtained by Rahimzadeh *et al.* (2015), who observed a dimming in Iran since the 2000s by analysing the surface synoptic measurements of sunshine hours. The findings of this study fit to the general picture that the widespread brightening in the 1990s has become less evident in the 2000s with a globally heterogeneous picture of regionally differing dimming and brightening trends (Wild *et al.,* 2009; Wild, 2012).

According to the results obtained in this study, despite the fact that CC only provides information about the horizontal extension of clouds (misses other properties of cloud) and measurement of CC mostly relies on

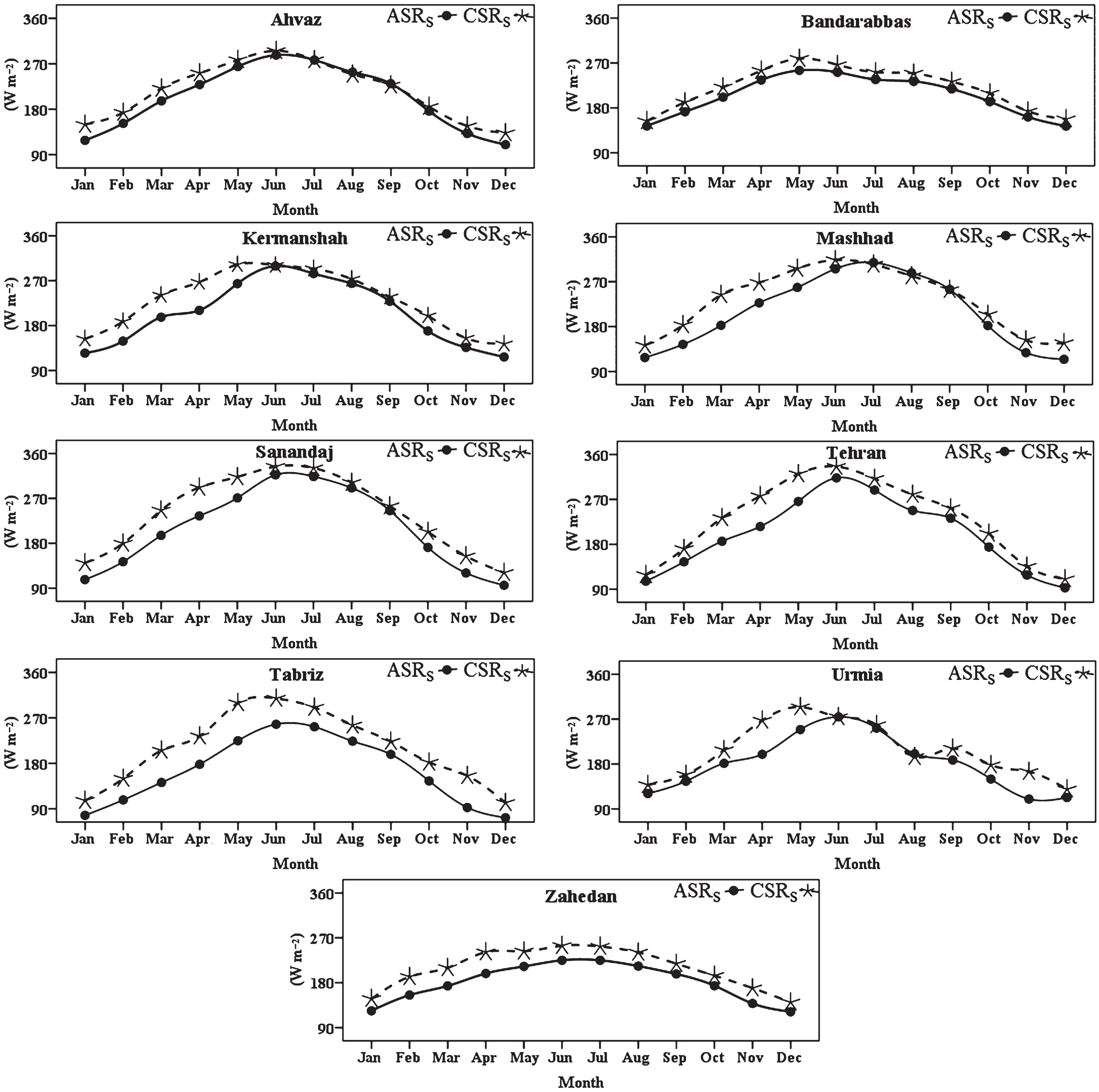

Figure 9. Long-term monthly averages of ASR_S and CSR_S for 1998–2015 at nine sites in Iran.

human judgments (there may be errors in measuring CC, especially when the amount of cloud is low), the dimming observed in Iran during 1998–2015 may to some extent be explained by increase in the amount of aerosol as well as variations in CC, either caused by interactions between CC and aerosols (indirect aerosol effects) or by natural variations unrelated to aerosol effects (Stanhill *et al.,* 2014; Mateos *et al.,* 2014; Storelvmo *et al.*, 2016; Tang *et al.,* 2017). This fact is supported by the evidence that the variations observed in CSR_S and CC overall seem to be in line with ASR_S during 1998–2015 (Figures 6 and 10). However, this may not be true for all of stations studied. Getting more precise, in terms of the station Tehran, for instance, ASR_S seems to have significantly (10% level) decreased ($\beta = -4.3$% per decade) over 1998–2015, while in contrast the amount of CC has not varied in line with ASR_S. Figure 7 also shows a lack of correlation between the mean annual values of ASR_S and CC measured at the station Tehran, but a strong positive correlation (non-significant) between ASR_S and CSR_S. This fact may be explained by the increase in the amount of aerosol in Tehran (Sabetghadam *et al.,* 2012; Crosbie *et al.,* 2014; Arhami *et al.,* 2017), which can notably affect the transparency of the atmosphere and therefor the amount of ASR_S received at this station (Sanchez-Lorenzo *et al.,* 2009; Wild, 2012; Zhao *et al.,* 2013; Sanchez-Romero *et al.,* 2014; Rahimzadeh *et al.,* 2015; Qian, 2016). Furthermore, it is worth to mention that aerosols in Tehran seem to largely origin from anthropogenic air pollution (Crosbie *et al.,* 2014; Sabetghadam and Ahmadi-Givi,

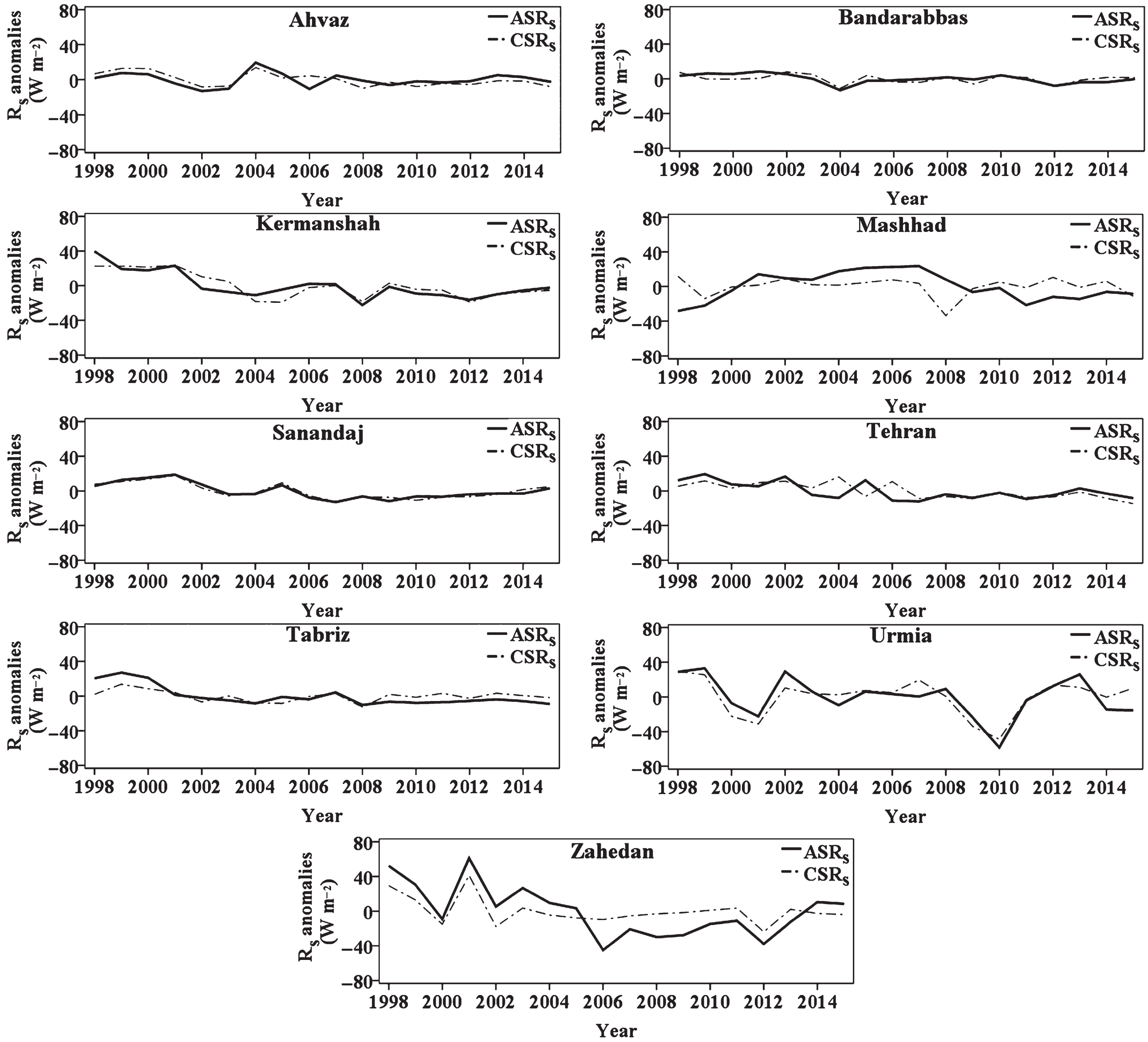

Figure 10. Anomalies of annual mean ASR_S and CSR_S during 1998–2015 at nine sites in Iran. Reference period for anomalies is also 1998–2015.

2014). The variations observed in CSR_S at the station Tehran also confirm this hypothesis because the trends observed in the time series of CSR_S show a significant decrease (1% level) of about −4.9% per decade, thus stronger than ASR_S. This fact may be explained by the decrease in the amount of CC ($\beta = -6.1\%$ per decade, significant at 1% level). In addition, the anomalies of ASR_S and CSR_S also show similar variation patterns during the study period.

In case of the station Ahvaz, as seen from Table 2 and Figure 2, ASR_S has also decreased by −0.8% per decade during the 2000s, which is in line with the variations of CSR_S and CC. However, Figure 7 shows a lack of significant correlation between ASR_S and CC, but a strong correlations between ASR_S and CSR_S. This may reveal the fact that ASR_S may have decreased as a result of combined effect of aerosol and CC or there may be other unknown driving factors causing dimming at the station Ahvaz. A more precise look through the long-term mean annual and monthly values and also the time series of CC shows that a great proportion of ASR_S at the station Ahvaz originates from CSR_S which may vary as a result of increase/decrease in the amount of aerosols. Recent studies with respect to aerosols show that dust and sand storms are frequent in the southwest of Iran (Cao *et al.,* 2015; Sarraf *et al.,* 2016; Middleton, 2017) and the highest amounts of aerosols is mostly observed during summer (Maleki *et al.,* 2016). This is mainly caused by sand and dust storms blowing from eastern Syria and Iraq (Shahsavani *et al.,* 2012; Amanollahi *et al.,* 2015), in addition to the dust activities originating from severe soil degradation in the Hoor-Al-Howizeh/Al-Azim marshes, which is mainly located in the Khuzestan province, in the southwest of Iran (Cao *et al.,* 2015) and has dried up as a consequence of several factors such as droughts, climate change, dam construction projects, etc. (Ali and Mahdi, 2008; Muhsin, 2011; Zarasvandi *et al.,* 2011). Furthermore, studies showed that the amount of dust born

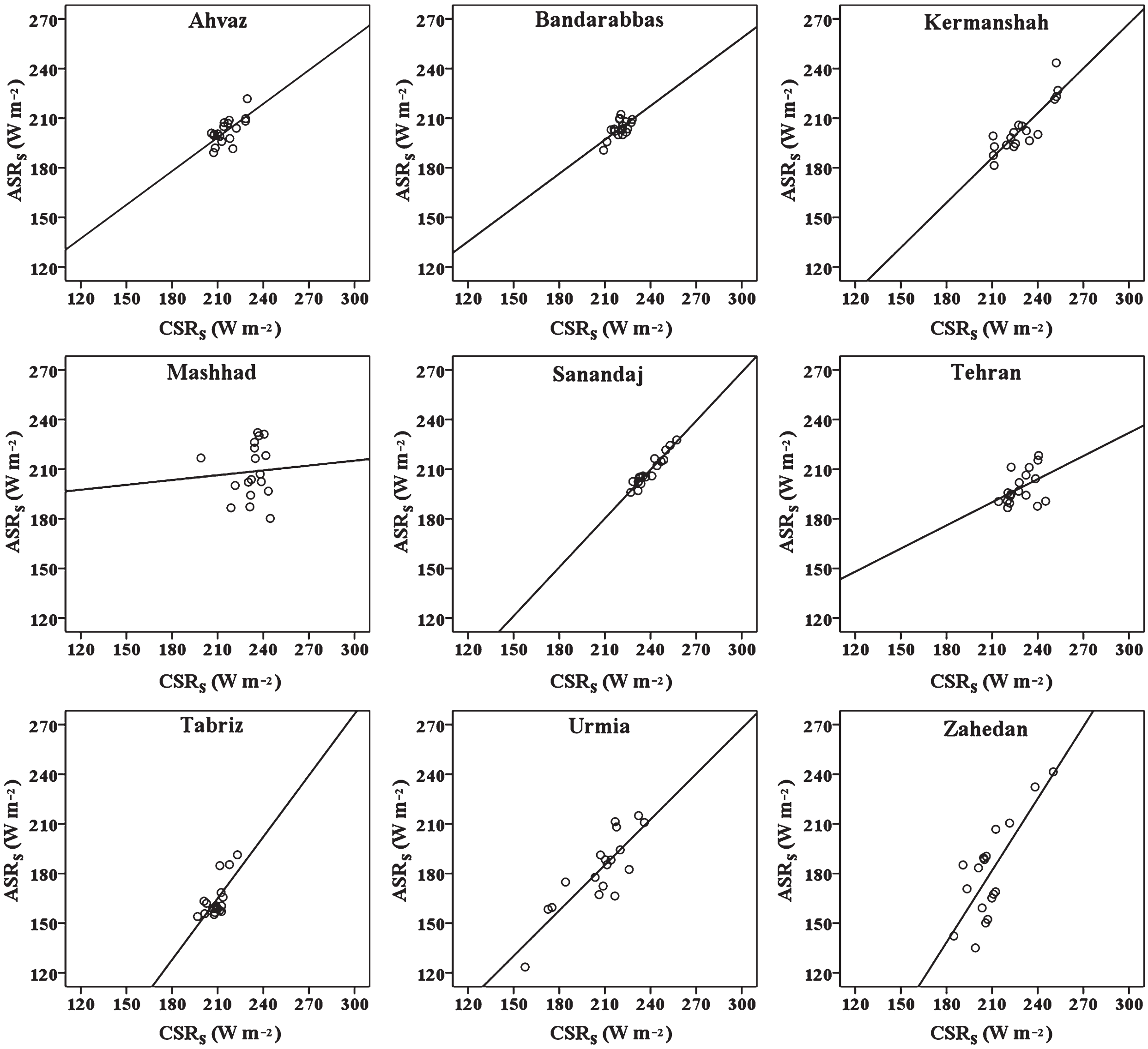

Figure 11. Scatterplots of the mean annual values of ASR_S *versus* CSR_S observed at each of the stations studied (note: the solid line represents the least square line fitted between the ASR_S and CSR_S observations).

aerosol in the southwest of Iran seems to have increased between 2000 and 2012, but decreased between 2012 and 2014 (Arndt *et al.,* 2010; Pozzer *et al.,* 2015; Klingmüller *et al.,* 2016; Mehta *et al.,* 2016; Namdar*i et al*., 2016). The results obtained in this study also show a decline of about −3.5% per decade (significant at 5%) in CSR_S at the station Ahvaz during the 2000s. Interestingly, the anomalies of CSR_S also show a decrease and an increase during 2000–2012 and 2012–2014, respectively. The slope of the increasing period, however, seems to be very small in comparison to the decreasing period. In addition to the dust/sand storms, variations in the amount of anthropogenic air pollution may be another factor, which may have affected the trends of ASR_S and CSR_S at the station Ahvaz. Ahvaz is typically an Agro-industrial city, surrounded by a great number of oil wells and companies and considered as one of the most polluted cities of the world (Maleki *et al.,* 2016). In addition, the time series of CC indicates a steep increase in the amount of CC ($\beta = 34.2\%$ per decade) at the station Ahvaz between 1998 and 2015. Overall, according to these facts, despite the fact that CSR_S and CC have both varied in line with ASR_S at the station Ahvaz (which is located at the capital of the Khuzestan province), variations of ASR_S during the study period seem to have been mostly governed by the changes in the amount of dust born aerosols during 1998–2015.

Furthermore, it is worth to mention that a lack of correlation between ASR_S and CSR_S was found at the station Mashhad (Figure 7). However, this may be explained by the absence of a monotonic trend in ASR_S and CC time series during the study period. According to the time-series plots provided in Figure 4, a transition from brightening to dimming was observed in ASR_S around the year 2007 at the station Mashhad, which was not detected in the CSR_S anomalies (Figure 10). Nevertheless, based on the correlation provided in Figure 7 and also the time series of CC illustrated in Figure 6, this transition seems to have occurred as a consequence of a decrease and increase observed in CC between 1998–2008 and 2009–2015, respectively. In addition, despite the fact that the overall variations of ASR_S ($\beta = -5.7\%$ per decade, significant at 1%) and CSR_S ($\beta = -0.9\%$ per decade, non-significant) point to the same direction, a comparison between the anomalies of ASR_S and CSR_S and also the correlations between these two variables (Figure 7) do not show a similar pattern of variation during the study period at this site (Figure 10). This may indicate that the inter-annual variations in ASR_S may be mostly explained by the variations in CC at this site.

In case of the station Zahedan, which is located in the southeast of Iran, a monotonic trend was neither observed. Based on the time series elaborated in Figure 4, ASR_S seems to have decreased between 1998 and 2006, but then started to increase until the end of the study period. However, the overall trend of ASR_S at the station Zahedan seems to be downward based on the MK method. Such a transition was not observed in the CC time series between 1998 and 2015 at the station Zahedan. This implies that the dimming and brightening periods observed at this station may not be explained by changes in CC. Instead, changes in the aerosols loading seems to be the potential reason, since, according to the data provided in Figure 2, a great proportion of the total annual ASR_S at the station Zahedan (the capital city of Sistan and Baluchestan province) originates from CSR_S (similar to station Ahvaz), which overall seems to have decreased by −1.7% per decade (insignificant) at this station. In addition, the studies with respect to aerosol activities in the southeast of Iran show that there is a high aerosol loading in the Sistan region during summer (Rashki *et al.,* 2013; Rashki *et al.,* 2014; Kaskaoutis *et al.,* 2015; Rashki *et al.,* 2015). This issue is mainly caused as a result of the strong 'Levar' winds in summer, which favour the uplift of large quantities of dust from the Hamoun basin (located in the northern part of Sistan and Baluchestan province) (Rashki *et al.,* 2012). Furthermore, it has been reported that dust aerosol loadings over the Sistan region have increased since the 2000s until 2004, but then decreased after 2004 (Rashki *et al.,* 2014). Thus, the transition from dimming to brightening observed at the station Zahedan may be a consequence of the increase and decrease in the amount of dust born aerosol loadings in the mentioned sub-periods, respectively. This transition from dimming to brightening around the year 2006 is also evident from the anomalies of CSR_S. Furthermore, the annual values of CSR_S also show a strong correlation with ASR_S at this station. In addition, the overall downward trend observed in ASR_S between 1998 and 2015 seems to be in line with the changes in dust-born aerosol loading together with a continuous increase in the amount of CC at the station Zahedan.

5. Conclusion

This study investigates the inter-annual and monthly trends of ASR_S, CSR_S and CC since the 2000s, by means of providing information on variations of R_s in Iran obtained from direct measurements, which have not previously been reported. To this aim, an overall number of nine stations across Iran were chosen, based on the availability of uniform R_s and CC records for the time period 1998–2015. The trends in the mentioned data were then analysed, using the modified MK and Sen's slope estimator methods. Based on the results obtained, the conclusions of this study can be summarized as follows:

- A great proportion of ASR_S in Iran is received during summer, when CC is minimal and the extraterrestrial solar input maximal. Specially in the south of Iran, where the annual amount of CC is relatively low, most of ASR_S received during summer originates from CSR_S.
- The overall variations observed in the directly measured values of R_s showed a widespread dimming phenomenon under both clear- and all-sky conditions with median magnitudes of −1.7 (CSR_S) and −4.3 (ASR_S) % per decade in Iran since the 2000s. This dimming was observed in all months of the year and seems to have occurred as a consequence of increase in the amount of aerosols loading and CC ($\beta = 20.0\%$ per decade). In the south of Iran and the station Tehran, the increase in the amount of aerosol loadings seems to play a more notable role in the decline in ASR_S in comparison with CC. The increase in the amount of aerosol loadings may originate from increase in anthropogenic air pollution as well as natural aerosols from dust storms, or caused by interactions between anthropogenic air pollution and natural aerosols.
- No monotonic variations were found in ASR_S at the stations located in the east of Iran, namely Mashhad and Zahedan. In case of the station Mashhad, a transition from brightening to dimming in the year 2007 was observed in ASR_S, which seems to be mainly caused by the decrease and increase in the amount of CC during 1998–2007 and 2007–2015, respectively, since this transition was not detected in the CSR_S time series. At the station Zahedan, in contrast, dimming and brightening in ASR_S were observed during 1998–2006 and 2006–2015, which may be explained by the increase and decrease of the dust aerosol loading during the mentioned sub-periods, respectively.

Acknowledgements

The authors appreciate the Islamic Republic of Iran's Meteorological Organization (IRIMO) for providing the required data. We also would like to kindly thank editor and the anonymous reviewers for their critical reviewing, which improved the work significantly.

References

Aladenola O, Madramootoo CA. 2014. Evaluation of solar radiation estimation methods for reference evapotranspiration estimation in Canada. *Theor. Appl. Climatol.* **118**: 377–385. https://doi.org/10.1007/s00704-013-1070-2.

Ali SM, Mahdi AS. 2008. Digital techniques for monitoring changes in water-body using satellite image. *Iraqi J. Sci.* **49**(1): 244–255.

Allen RG, Pereira LS, Raes D, Smith M. 1998. *Crop evapotranspiration – guidelines for computing crop water requirements*. FAO Irrigation and drainage paper 56. Food and Agriculture Organization: Rome.

Alpert P, Kishcha P, Kaufman YJ, Schwarzbard R. 2005. Global dimming or local dimming?: effect of urbanization on sunlight availability. *Geophys. Res. Lett.* **32**(17): L17802. https://doi.org/10.1029/2005GL023320.

Amanollahi J, Kaboodvandpour S, Qhavami S, Mohammadi B. 2015. Effect of the temperature variation between Mediterranean Sea and Syrian deserts on the dust storm occurrence in the western half of Iran. *Atmos. Res.* **154**: 116–125. https://doi.org/10.1016/j.atmosres.2014.11.003.

Arhami M, Hosseini V, Shahne MZ, Bigdeli M, Lai A, Schauer JJ. 2017. Seasonal trends, chemical speciation and source apportionment of fine PM in Tehran. *Atmos. Environ.* **31**(153): 70–82. https://doi.org/10.1016/j.atmosenv.2016.12.046.

Arndt DS, Baringer MO, Johnson MR (eds). 2010. State of the climate in 2009. *Bull. Am. Meteorol. Soc.* **91**(7): S1–S224. https://doi.org/10.1175/BAMS-91-7-StateoftheClimate.

Calbo J, Gonzalez JA, Sanchez-Lorenzo A. 2016. Building global and diffuse solar radiation series and assessing decadal trends in Girona (NE Iberian Peninsula). *Theor. Appl. Climatol.* **10**: 1–13. https://doi.org/10.1007/s00704-016-1829-3.

Cao H, Liu J, Wang G, Yang G, Luo L. 2015. Identification of sand and dust storm source areas in Iran. *J. Arid. Land* **7**(5): 567–578. https://doi.org/10.1007/s40333-015-0127-8.

Chiacchio M, Solmon F, Giorgi F, Stackhouse P, Wild M. 2015. Evaluation of the radiation budget with a regional climate model over Europe and inspection of dimming and brightening. *J. Geophys. Res. Atmos.* **120**(5): 1951–1971. https://doi.org/10.1002/2014JD022497.

Chin M, Diehl TL, Bian H, Yu H, Qian Y, Wild M, Streets DG, Stackhouse PW. 2014. Multi-decadal trends of solar radiation reaching the surface: what is the role of aerosols? In *AGU Fall Meeting Abstracts*, AGU, San Francisco, California, 1 December 2014.

Crosbie E, Sorooshian A, Monfared NA, Shingler T, Esmaili O. 2014. A multi-year aerosol characterization for the greater Tehran area using satellite, surface, and modeling data. *Atmos.* **5**(2): 178–197. https://doi.org/10.3390/atmos5020178.

Dagon K, Schrag DP. 2016. Exploring the effects of solar radiation management on water cycling in a coupled land–atmosphere model. *J. Clim.* **29**(7): 2635–2650. https://doi.org/10.1175/JCLI-D-15-0472.1.

Demirhan H, Atilgan YK. 2015. New horizontal global solar radiation estimation models for Turkey based on robust cop lot supported genetic programming technique. *Energy Convers. Manag.* **106**: 1013–1023. https://doi.org/10.1016/j.enconman.2015.10.038.

Dinpashoh Y, Jhajharia D, Fakheri-Fard A, Singh VP, Kahya E. 2011. Trends in reference crop evapotranspiration over Iran. *J. Hydrol.* **399**: 422–433. https://doi.org/10.1016/j.jhydrol.2011.01.021.

Dong SX, Davis SJ, Ashton PS, Bunyavejchewin S, Nur Supaedi MN, Kassim AR, Tan S, Moorcroft P. 2012. Variability of solar radiation and temperature explains observed patterns and trends in tree growth rates across four tropical forests. *Proc. R. Soc. B* **279**: 3923–3931. https://doi.org/10.1098/rspb.2012.1124.

El Mghouchi Y, El Bouardi A, Sadouk A, Fellak I, Ajzoula T. 2016. Comparison of three solar radiation models and their validation under all sky conditions – case study: Tetuan city in northern of Morocco. *Renew. Sust. Energ. Rev.* **58**: 1432–1444. https://doi.org/10.1016/j.rser.2015.12.354.

Huber I, Bugliaro L, Ponater M, Garny H, Emde C, Mayer B. 2016. Do climate models project changes in solar resources? *Sol. Energy* **129**: 65–84. https://doi.org/10.1016/j.solener.2015.12.016.

Jaagus J. 2006. Climatic changes in Estonia during the second half of the 20th century in relationship with changes in large-scale atmospheric circulation. *Theor. Appl. Climatol.* **83**: 77–88. https://doi.org/10.1007/s00704-005-0161-0.

Jahani B, Mohammadi AS, Albaji M. 2016. Impact of climate change on crop water and irrigation requirement (case study: eastern Dez Plain, Iran). *Polish J. Nat. Sci.* **31**(2): 151–167.

Jahani B, Dinpashoh Y, Raisi NA. 2017. Evaluation and development of empirical models for estimating daily solar radiation. *Renew. Sust. Energ. Rev.* **73**: 878–891. https://doi.org/10.1016/j.rser.2017.01.124.

Kaskaoutis DG, Rashki A, Houssos EE, Mofidi A, Goto D, Bartzokas A, Francois P, Legrand M. 2015. Meteorological aspects associated with dust storms in the Sistan region, southeastern Iran. *Clim. Dyn.* **45**(1–2): 407–424. https://doi.org/10.1007/s0038.

Kendall MG. 1975. *Rank Correlation Methods*, 4th edn. Charles Griffin: London.

Klingmüller K, Pozzer A, Metzger S, Stenchikov GL, Lelieveld J. 2016. Aerosol optical depth trend over the Middle East. *Atmos. Chem. Phys.* **16**(8): 5063–5073. https://doi.org/10.5194/acp-16-5063-2016.

Kumar S, Merwade V, Kam J, Thurner K. 2009. Streamflow trends in Indiana: effects of long term persistence, precipitation and subsurface drains. *J. Hydrol.* **374**(1–2): 171–183. https://doi.org/10.1016/j.jhydrol.2009.06.012.

Kumari BP, Londhe A, Daniel S, Jadhav DB. 2007. Observational evidence of solar dimming: offsetting surface warming over India. *Geophys. Res. Lett.* **34**(21): L21810. https://doi.org/10.1029/2007GL031133.

Kun Y, Koike T, Ye B. 2006. Improving estimation of hourly, daily, and monthly solar radiation by importing global data sets. *Agric. For. Meteorol.* **137**: 43–55. https://doi.org/10.1016/j.agrformet.2006.02.001.

Lindfors AV, Kouremeti N, Arola A, Kazadzis S, Bias AF, Laaksonen A. 2013. Effective aerosol optical depth from pyranometer measurements of surface solar radiation (global radiation) at Thessaloniki, Greece. *Atmos. Chem. Phys.* **13**: 3733–3741. https://doi.org/10.5194/acp-13-3733-2013.

Longman RJ, Giambelluca TW, Alliss R, Barnes ML. 2014. Temporal solar radiation change at high elevations in Hawai'i. *J. Geophys. Res. Atmos.* **119**: 6022–6033. https://doi.org/10.1002/2013JD021322.

Maleki H, Sorooshian A, Goudarzi G, Nikfal A, Baneshi MM. 2016. Temporal profile of PM 10 and associated health effects in one of the most polluted cities of the world (Ahvaz, Iran) between 2009 and 2014. *Aeolian Res.* **22**: 135–140. https://doi.org/10.1016/j.aeolia.2016.08.006.

Manara V, Brunetti M, Celozzi A, Maugeri M, Sanchez-Lorenzo A, Wild M. 2016. Detection of dimming/brightening in Italy from homogenized all-sky and clear-sky surface solar radiation records and underlying causes (1959–2013). *Atmos. Chem. Phys.* **16**(17): 11145–11161. https://doi.org/10.5194/acp-16-11145-2016.

Mann HB. 1945. Non-parametric tests against trend. *Econometrica* **33**: 245–259.

Mateos D, Sanchez-Lorenzo A, Antón M, Cachorro VE, Calbó J, Costa MJ, Torres B, Wild M. 2014. Quantifying the respective roles of aerosols and clouds in the strong brightening since the early 2000s over the Iberian Peninsula. *J. Geophys. Res. Atmos.* **119**(17): 10382–10393. https://doi.org/10.1002/2014JD022076.

Mehta M, Singh R, Singh A, Singh N. 2016. Recent global aerosol optical depth variations and trends – a comparative study using MODIS and MISR level 3 datasets. *Remote Sens. Environ.* **181**: 137–150. https://doi.org/10.1016/j.rse.2016.04.004.

Middleton NJ. 2017. Desert dust hazards: a global review. *Aeolian Res.* **24**: 53–63. https://doi.org/10.1016/j.aeolia.2016.12.001.

Moghaddasi M, Morid S, Delavar M, Hossaini SH. 2017. Lake Urmia Basin drought risk management: a trade-off between environment and agriculture. *Irrig. Drain.* **66**: 439–450. https://doi.org/10.1002/ird.2112.

Muhsin IJ. 2011. Al-hawizeh marsh monitoring method using remotely sensed images. *Iraqi J. Sci.* **52**(3): 381–387.

Müller B, Wild M, Driesse A, Behrens K. 2014. Rethinking solar resource assessments in the context of global dimming and brightening. *Sol. Energy* **99**: 272–282. https://doi.org/10.1016/j.solener.2013.11.013.

Namdari S, Valizade KK, Rasuly AA, Sarraf BS. 2016. Spatio-temporal analysis of MODIS AOD over western part of Iran. *Arab. J. Geosci.* **9**(3): 1–11. https://doi.org/10.1007/s1251.

Ohmura A, Lang H. 1989. In *IRS'88: Current Problems in Atmospheric Radiation*, Lenoble J, Geleyn J-F (eds). Deepak Publishing: Hampton, VA.

Pinker RT, Zhang B, Dutton EG. 2005. Do satellites detect tends in surface solar radiation? *Science* **308**(5723): 850–854. https://doi.org/10.1126/science.1103159.

Power HC. 2003. Trends in solar radiation over Germany and an assessment of the role of aerosols and sunshine duration. *Theor. Appl. Climatol.* **76**(1): 47–63. https://doi.org/10.1007/s00704-003-0005-8.

Pozzer A, de Meij A, Yoon J, Tost H, Georgoulias AK, Astitha M. 2015. AOD trends during 2001–2010 from observations and model simulations. *Atmos. Chem. Phys.* **15**(10): 5521–5535. https://doi.org/10.5194/acp-15-5521-2015.

Qian C. 2016. Impact of land use/land cover change on changes in surface solar radiation in eastern China since the reform and opening up. *Theor. Appl. Climatol.* **123**(1): 131–139. https://doi.org/10.1007/s00704-014-1334-5.

Qian Y, Kaiser DP, Leung LR, Xu M. 2006. More frequent cloud-free sky and less surface solar radiation in China from 1955 to 2000. *Geophys. Res. Lett.* **33**: L01812. https://doi.org/10.1029/2005GL024586.

Quej VH, Almorox J, Ibrakhimov M, Saito L. 2017. Estimating daily global solar radiation by day of the year in six cities located in the

Yucatán Peninsula, Mexico. *J. Clean. Prod.* **141**: 75–82. https://doi.org/10.1016/j.jclepro.2016.09.062.

Rahimzadeh F, Sanchez-Lorenzo A, Hamedi M, Kruk MC, Wild M. 2015. New evidence on the dimming/brightening phenomenon and decreasing diurnal temperature range in Iran (1961–2009). *Int. J. Climatol.* **35**(8): 2065–2079. https://doi.org/10.1002/joc.4107.

Ramanathan V, Ramana MV, Roberts G, Kim D, Corrigan C, Chung C, Winker D. 2007. Warming trends in Asia amplified by brown cloud solar absorption. *Nature* **448**: 575–578. https://doi.org/10.1038/nature06019.

Rashki A, Kaskaoutis DG, Eriksson PG, Qiang M, Gupta P. 2012. Dust storms and their horizontal dust loading in the Sistan region, Iran. *Aeolian Res.* **5**: 51–62. https://doi.org/10.1016/j.aeolia.2011.12.001.

Rashki A, deW Rautenbach CJ, Eriksson PG, Kaskaoutis DG, Gupta P. 2013. Temporal changes of particulate concentration in the ambient air over the city of Zahedan, Iran. *Air Qual. Atmos. Health* **6**(1): 123–135. https://doi.org/10.1007/s11869-011-0152-5.

Rashki A, Kaskaoutis DG, Eriksson PG, Rautenbach CD, Flamant C, Vishkaee FA. 2014. Spatio-temporal variability of dust aerosols over the Sistan region in Iran based on satellite observations. *Nat. Hazards* **71**(1): 563–585. https://doi.org/10.1007/s11069-013-0927-0.

Rashki A, Kaskaoutis DG, Francois P, Kosmopoulos PG, Legrand M. 2015. Dust-storm dynamics over Sistan region, Iran: seasonality, transport characteristics and affected areas. *Aeolian Res.* **16**: 35–48. https://doi.org/10.1016/j.aeolia.2014.10.003.

Sabetghadam S, Ahmadi-Givi F. 2014. Relationship of extinction coefficient, air pollution, and meteorological parameters in an urban area during 2007 to 2009. *Environ. Sci. Pollut. Res. Int.* **21**(1): 538. https://doi.org/10.1007/s11356-013-1901-9.

Sabetghadam S, Ahmadi-Givi F, Golestani Y. 2012. Visibility trends in Tehran during 1958-2008. *Atmos. Environ.* **62**: 512–520. https://doi.org/10.1016/j.atmosenv.2012.09.008.

Sanchez-Lorenzo A, Wild M. 2012. Decadal variations in estimated surface solar radiation over Switzerland since the late 19th century. *Atmos. Chem. Phys.* **12**(18): 8635–8644. https://doi.org/10.5194/acp-12-8635-2012.

Sanchez-Lorenzo A, Calbo J, Brunetti M, Deser C. 2009. Dimming/brightening over the Iberian Peninsula: trends in sunshine duration and cloud cover, and their relations with atmospheric circulation. *J. Geophys. Res.* **114**: D00D09. https://doi.org/10.1029/2008JD011394.

Sanchez-Lorenzo A, Calbo J, Wild M. 2013. Global and diffuse solar radiation in Spain: building a homogeneous dataset and assessing their trends. *Glob. Planet. Chang.* **100**: 343–352. https://doi.org/10.1016/j.gloplacha.2012.11.010.

Sanchez-Lorenzo A, Mateos D, Wild M, Calbo J, Anton M, Enriquez-Alonso A, Sanchez-Romero A. 2014. Trends in solar radiation in Spain since 1980s: the role of the changes in the radiative effects of aerosols and clouds. *Geophys. Res. Abstr.* **16**: EGU2014–EG11345.

Sanchez-Lorenzo A, Wild M, Brunetti M, Guijarro JA, Hakuba MZ, Calbó J, Mystakidis S, Bartok B. 2015. Reassessment and update of long-term trends in downward surface shortwave radiation over Europe (1939–2012). *J. Geophys. Res. Atmos.* **120**(18): 9555–9569. https://doi.org/10.1002/2015JD023321.

Sanchez-Lorenzo A, Enriquez-Alonso A, Wild M, Trentmann J, Vicente-Serrano SM, Sanchez-Romero A, Posselt R, Hakuba MZ. 2017. Trends in downward surface solar radiation from satellites and ground observations over Europe during 1983–2010. *Remote Sens. Environ.* **189**: 108–117. https://doi.org/10.1016/j.rse.2016.11.018.

Sanchez-Romero A, Sanchez-Lorenzo A, Calbó J, González JA, Azorin-Molina C. 2014. The signal of aerosol-induced changes in sunshine duration records: a review of the evidence. *J. Geophys. Res. Atmos.* **119**(8): 4657–4673. https://doi.org/10.1002/2013JD021393.

Sarraf BS, Rasouli AA, Mohammadi GH, Sadr AH. 2016. Long-term trends of seasonal dusty day characteristics – West Iran. *Arab. J. Geosci.* **9**(10): 563–571. https://doi.org/10.1007/s12517-016-2589-1.

Sen PK. 1968. Estimates of the regression coefficients based on Kendall's tau. *J. Am. Stat. Assoc.* **63**: 1379–1389.

Shadkam S, Ludwig F, van Vliet MT, Pastor A, Kabat P. 2016a. Preserving the world second largest hypersaline lake under future irrigation and climate change. *Sci. Total Environ.* **559**: 317–325. https://doi.org/10.1016/j.scitotenv.2016.03.190.

Shadkam S, Ludwig F, van Oel P, Kirmit Ç, Kabat P. 2016b. Impacts of climate change and water resources development on the declining inflow into Iran's Urmia Lake. *J. Great Lakes Res.* **42**(5): 942–952. https://doi.org/10.1016/j.jglr.2016.07.033.

Shahsavani A, Naddafi K, Haghighifard NJ, Mesdaghinia A, Yunesian M, Nabizadeh R, Arahami M, Sowlat MH, Yarahmadi M, Saki H, Alimohamadi M. 2012. The evaluation of PM 10, PM 2.5, and PM 1 concentrations during the Middle Eastern Dust (MED) events in Ahvaz, Iran, from April through September 2010. *J. Arid Environ.* **77**: 72–83. https://doi.org/10.1016/j.jaridenv.2011.09.007.

Soni VK, Pandithuai G, Pai DS. 2012. Evaluation of long-term changes of solar radiation in India. *Int. J. Climatol.* **32**: 540–551. https://doi.org/10.1002/joc.2294.

Stanhill G, Achiman O, Rosa R, Cohen S. 2014. The cause of solar dimming and brightening at the Earth's surface during the last half century: evidence from measurements of sunshine duration. *J. Geophys. Res. Atmos.* **119**(18): 10902–10911. https://doi.org/10.1002/2013JD021308.

Stone R. 2015. Saving Iran's Great Salt Lake. *Science* **349**(6252): 1044–1047. https://doi.org/10.1126/science.349.6252.1044.

Storelvmo T, Leirvik T, Lohmann U, Phillips PCB, Wild M. 2016. Disentangling greenhouse warming and aerosol cooling to reveal Earth's climate sensitivity. *Nat. Geosci.* **9**(4):286–289. https://doi.org/10.1038/ngeo2670.

Tabari H, Hosseinizadeh Talaee P. 2011. Temporal variability of precipitation over Iran: 1966-2005. *J. Hydrol.* **396**: 313–320. https://doi.org/10.1016/j.jhydrol.2010.11.034.

Tang W, Yang K, He J, Qin J. 2010. Quality control and estimation of global solar radiation in China. *Sol. Energy* **84**(3): 466–475. https://doi.org/10.1016/j.solener.2010.01.006.

Tang WJ, Yang K, Qin J, Cheng CC, He J. 2011. Solar radiation trend across China in recent decades: a revisit with quality-controlled data. *Atmos. Chem. Phys.* **11**(1): 393–406. https://doi.org/10.5194/acp-11-393-2011.

Tang W, Yang K, Qin J, Niu X, Lin C, Jing X. 2017. A revisit to decadal change of aerosol optical depth and its impact on global radiation over China. *Atmos. Environ.* **150**: 106–115. https://doi.org/10.1016/j.atmosenv.2016.11.043.

Theil H. 1950. A rank invariant method of linear and polynomial regression analysis, part 3. *Proc. R. Netherlands Acad. Sci.* **53**: 1397–1412.

Viorel B. 2008. *Modeling Solar Radiation at the Earth Surface*. Springer: Berlin Heidelberg.

Von Schuckmann K, Palmer MD, Trenberth KE, Cazenave A, Chambers D, Champollion N, Hansen J, Josey SA, Loeb N, Mathieu PP, Meyssignac B. 2016. An imperative to monitor Earth's energy imbalance. *Nat. Clim. Chang.* **6**(2): 138–144. https://doi.org/10.1038/nclimate2876.

Wang Y, Wild M. 2016. A new look at solar dimming and brightening in China. *Geophys. Res. Lett.* **43**: 11777–11785. https://doi.org/10.1002/2016GL071009.

Wang K, Dickinson RE, Wild M, Liang SE. 2012. Atmospheric impacts on climatic variability of surface incident solar radiation. *Atmos. Chem. Phys.* **12**: 9581–9592. https://doi.org/10.5194/acp-12-9581-2012.

Wang YW, Wild M, Sanchez-Lorenzo A, Yang Y, Manara V, Ren D. 2016. Urbanization effect on sunshine duration during global dimming and brightening periods in China. *Atmos. Chem. Phys. Discuss.* **2016**: 1–20. https://doi.org/10.5194/acp-2016-657.

Wang J, Dong J, Wang S, Zhang L, He H, Yi Y, Lu G, Oyler J, Smith WK, Zhao M, Yu G. 2017. Decreasing net primary production due to drought and slight decreases in solar radiation in China from 2000 to 2012. *J. Geophys. Res. Biogeosci.* **122**(1): 261–278. https://doi.org/10.1002/2016JG003417.

Wild M. 2009. Global dimming and brightening: a review. *J. Geophys. Res.* **114**: D00D16. https://doi.org/10.1029/2008JD011470.

Wild M. 2012. Enlightening global dimming and brightening. *Bull. Am. Meteorol. Soc.* **93**: 27–37. https://doi.org/10.1175/BAMS-D-11-00074.1.

Wild M, Gilgen H, Roesch A, Ohmura A, Long CN, Dutton EG, Forgan B, Kallis A, Russak V, Tsvetkov A. 2005. From dimming to brightening: decadal changes in solar radiation at Earth's surface. *Science* **308**: 847–850. https://doi.org/10.1126/science.110321.

Wild M, Trüssel B, Ohmura A, Long CN, König-Langlo G, Dutton EG, Tsvetkov A. 2009. Global dimming and brightening: an update beyond 2000. *J. Geophys. Res.* **114**: D00D13. https://doi.org/10.1029/2008JD011382.

Wild M, Folini D, Henschel F, Fischer N, Müller B. 2015a. Projections of long-term changes in solar radiation based on CMIP5 climate models and their influence on energy yields of photovoltaic systems. *Sol. Energy* **116**: 12–24. https://doi.org/10.1016/j.solener.2015.03.039.

Wild M, Folini D, Hakuba MZ, Schär C, Seneviratne SI, Kato S, Rutan D, Ammann C, Wood EF, König-Langlo G. 2015b. The energy balance over land and oceans: an assessment based on direct observations and

CMIP5 climate models. *Clim. Dyn.* **44**(11–12): 3393–3429. https://doi.org/10.1007/s00382-014-2430-z.

Xia XA, Wang PC, Chen HB, Liang F. 2006. Analysis of downwelling surface solar radiation in China from National Centers for Environmental Prediction Reanalysis, Satellite Estimates, And Surface Observations. *J. Geophys. Res.* **111**(D9): D09103. https://doi.org/10.1029/2005JD006405.

Yang X, Zhao C, Zhou L, Wang Y, Liu X. 2016. Distinct impact of different types of aerosols on surface solar radiation in China. *J. Geophys. Res. Atmos.* **121**(11): 6459–6471. https://doi.org/10.1002/2016JD024938.

Zarasvandi A, Carranza EJ, Moore F, Rastmanesh F. 2011. Spatio-temporal occurrences and mineralogical–geochemical characteristics of airborne dusts in Khuzestan Province (southwestern Iran). *J. Geochem. Explor.* **111**(3): 138–151. https://doi.org/10.1016/j.gexplo.2011.04.004.

Zekai S. 2008. *Solar Energy Fundamentals and Modeling Techniques: Atmosphere, Environment, Climate Change and Renewable Energy*. Springer: London.

Zhao N, Zeng X, Han S. 2013. Solar radiation estimation using sunshine hour and air pollution index in China. *Energy Convers. Manag.* **76**: 846–851. https://doi.org/10.1016/j.enconman.2013.08.037.